VOL. 9, NO. 6, JUNE 2014 ISSN 1819-6608
ARPN Journal of Engineering and Applied Sciences


www.arpnjournals.com

CYCLE ANALYSIS OF LINEAR COMPRESSORS USING THREE-DIMENSIONAL CFD

I. Y. An and Y. L. Lee
Department of Mechanical Engineering, Kongju National University, Korea
E-Mail: ylee@kongju.ac.kr

ABSTRACT

In order to improve the efficiency of the refrigeration cycle or the heat pump cycle, it is important to improve the efficiency of a compressor. In this study, the authors intended to develop a three-dimensional numerical model that can predict the performance of a linear compressor. For this purpose, CFD model which can simulate the entire cycle was developed. The numerical analysis on the cooling capacity of two linear compressors was successfully conducted and the numerical results were in good agreement with the experimental results. In future, if considering the detailed valve behavior, the accuracy of the numerical analysis model can be further improved.

Keywords: linear compressor, cooling capacity, CFD, cycle analysis.

INTRODUCTION

Refrigerators, air conditioners and heat pumps, etc. using a refrigeration cycle are providing various conveniences and the comfort of life. However, these products require much electric energy, and in particular, the refrigerator uses about 20-40% of the electric energy used in the home. In addition, the compressor constituting the refrigerator consumes about 80% of the total electricity required by the refrigerator [1]. Thus, improving the compressor efficiency can be an efficient way to save energy.

The reciprocating compressor having high reliability and good efficiency has been commonly used as the compressor for a refrigerator or a heat pump long. However, because the efficiency of the reciprocating compressor is relatively low, the need for higher efficiency compressor is increasing. One of such high-efficiency compressors is just the linear compressor. Since the linear compressor uses the magnet with high magnetic force as a motor, the crank structure required in the reciprocating compressor does not need. This linear compressor has about 24% higher efficiency in comparison with the reciprocating compressor since it has not only small friction loss and wear but also low flow resistance [2].

Many studies have been conducted since the linear compressor has higher efficiency than the reciprocating compressor. Kim and Jeong [3, 4] have studied the performance characteristics of ICM (Inherent Capacity Modulated) linear compressor for the refrigerator through the numerical analysis and the experiments, and Kim *et al*., [5] have studied the dynamic characteristics with the numerical analysis and the experiments. Bradshaw *et al*., [6] have studied on the comprehensive model of the small linear compressor for electronics cooling, and Chen *et al*., [7] have studied on the magnetic-field distribution of the linear motor. Tsai and Chiang [8] have studied on MLLA (Magnetically Levitated Linear Actuator) of the linear compressor through the numerical analysis and the experiments, and Yang and Huang [9] have studied on the double fuzzy regulators for the phase or the stroke of the linear compressor of the Stirling cryogenic refrigerator.

However, the development of a higher efficiency linear compressor is necessary in accordance with the needs of consumers such as more various design, specialized functions and large capacity. Recently, the need for the flow optimization of the linear compressor using CFD (Computational Fluid Dynamics) has arisen to further improve the efficiency.

In this study, the numerical model that can simulate the entire cycle of the linear compressor including compression and expansion processes has been developed. Then, the numerical analysis on the cooling capacity of two linear compressors was conducted, and the numerical model was verified through the experiments. Therefore, this numerical model can be successfully used for further improving or optimizing the performance of a linear compressor. Fluent [10] was adopted for CFD simulations with user defined functions.

NUMERCAL ANALYSIS AND EXPERIMENTAL METHODS

Governing equations and mesh system

The flow of the fluid considered in this study is three-dimensional, compressible and unsteady, and realizable k-ε turbulent model proposed by Shinh *et al*., [11] was used. In addition, the standard wall functions proposed by Launder and Spalding [12] were used for the near-wall treatment. The Reynolds Averaged Navier-Stokes (RANS) equation and the energy equation used in the numerical analysis can be found elsewhere. [10]

Figure-1 shows the mesh system for the flow analysis of the linear compressor model. Since three-dimensional, compressible, unsteady and turbulent flow requires generally lots of computing time, the number of cells for the numerical model was minimized as possible. In this case, about 120, 000 cells were used in the model-1, and 170, 000 cells were used in the model-2. Also, the hybrid mesh system that consists of tetrahedral,

hexahedral, prism and pyramid cells was used as shown in Figure-2.

Cycle modeling of linear compressors

The numerical analysis has been performed over the entire cycle including the compression and expansion processes. Initially the piston is located at BDC (Bottom Dead Center), and the piston moves by 12.4mm compressing the cylinder when the suction valve and the discharge valve are closed. Next, the discharge valve opens and discharges the refrigerant, and the discharge valve, then, is closed again while it reaches the TDC (Top Dead Center). Thereafter, the expansion process starts and the suction valve opens when the pressure of the cylinder becomes low enough, allowing the refrigerant to flow into the cylinder. Finally, when the piston reaches the BDC, the suction valve is closed and a whole cycle is over. The numerical analysis repeats this cycle.

Figure-3 shows the cutting planes of two compressor models used in the numerical analysis. The two models are different each other in terms of piston movement. In the case of model-1, the copper pipe connected from the evaporator is fixed inside the piston, and because there is the gap between the piston and the pipe, the cylinder is compressed only by the piston movement. On the other hand, in the case of the model-2, the cylinder is compressed by both movements of the piston and the pipe since the piston and the pipe are stuck each other as an integral system. The opening time of the discharge valve was assumed as the moment that the pressure of cylinder becomes greater than 416.030 Pa during the compression process. In the numerical analysis, the boundary condition of the discharge valve was simply changed from wall to pressure outlet. After that, when the piston is reached the TDC, the boundary condition of the discharge valve is changed back from pressure outlet to wall. The opening time of the suction valve was assumed as the moment that the cylinder side pressure of the suction valve becomes smaller than the piston side pressure. The boundary condition of the suction valve is changed from wall to interior and consequently the refrigerant can be flowed into a cylinder. And then, when the piston is again reached BDC, the suction valve is closed. Opening and closing times of the suction valve and the discharge valve during a cycle are summarized in Table-1.

Table-1. Cycle events modeling.

Events	Events conditions	BC change
Open discharge valve	If P@cylinder ≥ 416,030Pa	Wall → Pressure outlet
Close discharge valve	If TDC	Pressure outlet→ Wall
Open suction valve	If P@svalve_cyl_side ≤ P@svalve_piston_side	Wall → interior
Close suction valve	If BDC	Interior → Wall

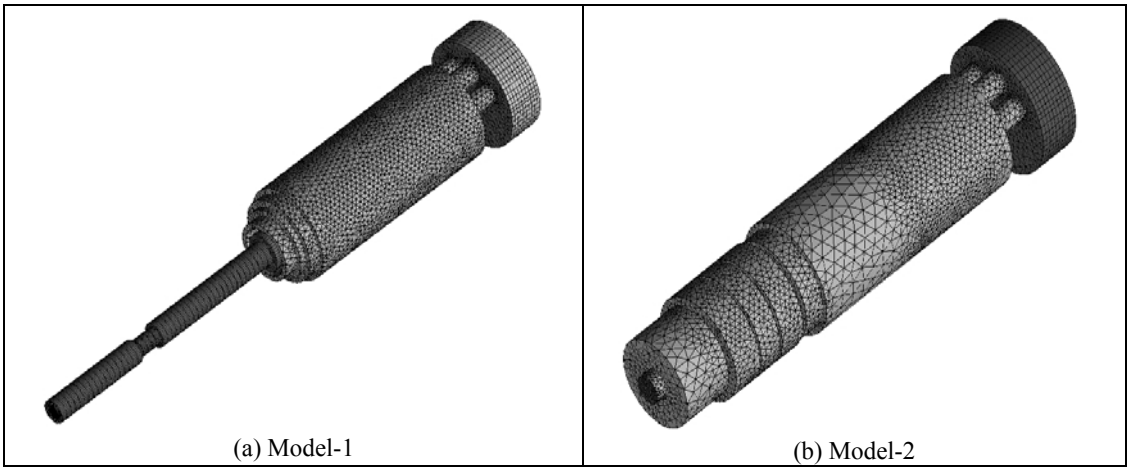

(a) Model-1 (b) Model-2

Figure-1. Mesh system for linear compressors.

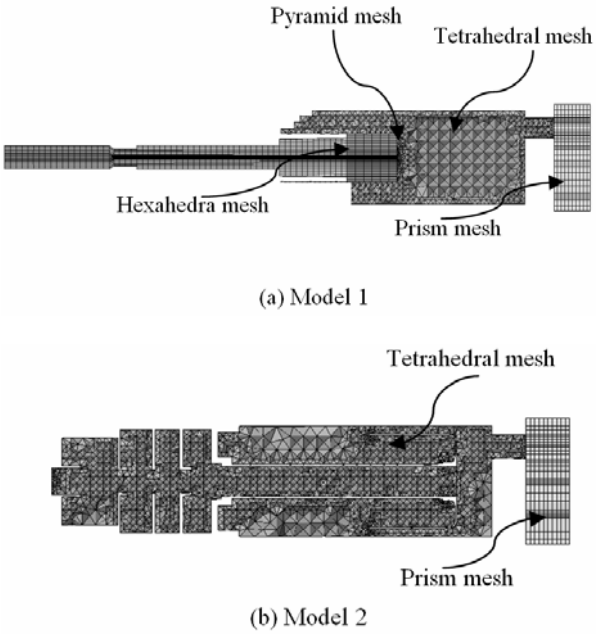

Figure-2. Mesh at the cross section.

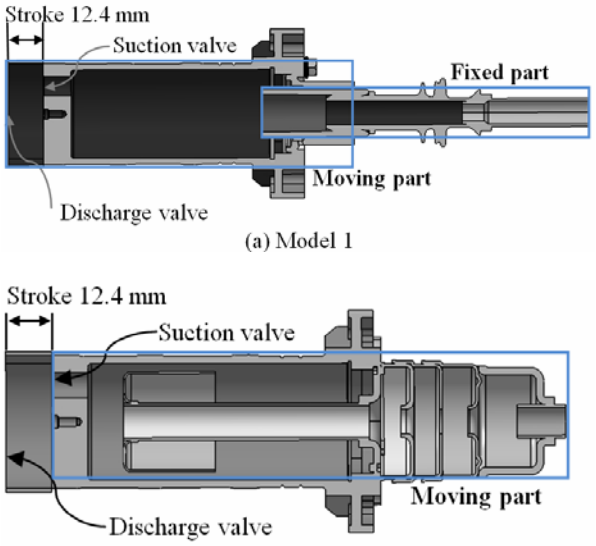

Figure-3. Cross sections for linear compressors.

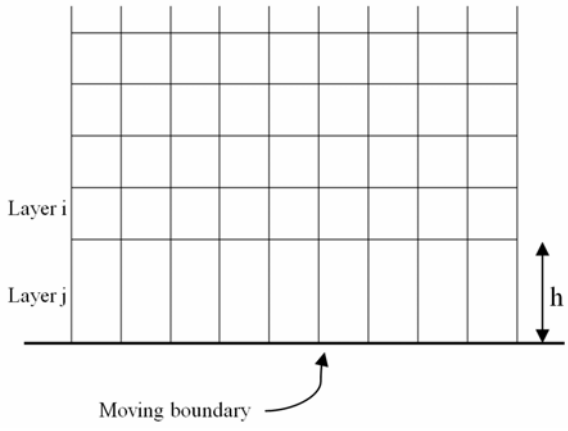

Figure-4. Dynamic layering [13].

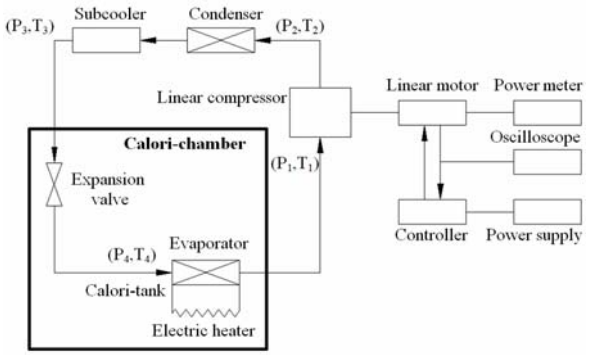

Figure-5. Experimental apparatus [6].

The fluid assumed in the numerical analysis is the isobutene (R600a) which is one of the real gas models provided by NIST (National Institute of Standards and Technology) (14) and it was assumed that the inlet pressure is 48,550 Pa, the discharge pressure 416, 030 Pa, the minimum clearance between the cylinder and the piston 0.04mm and the number of frequency 56.5 Hz. Also, the cooling capacity Q_{CC} in the numerical analysis was calculated from equation (1).

$$Q_{CC} = m_{avg} \times (h_1 - h_4) \quad (1)$$

Dynamic mesh method

In this study, the layering method among dynamic mesh methods was adopted in order to analyze the performance of the linear compressor. The layering method adds and removes layers of cells adjacent to a moving boundary, based on the height of the layer adjacent to the moving surface as shown in Figure-4. This technique is considerably accurate to describe the behavior of the linear compressor that repeats a simple, linear motion. Equation (2) and (3) show the split and the merge relationships in dynamic layering.

$$h_{min} > (1+\alpha_s) h_{ideal} \quad (2)$$

$$h_{max} < \alpha_c h_{ideal} \quad (3)$$

where, h_{min} is the minimum cell height of cell layer, h_{max} is the maximum cell height, h_{ideal} is an ideal cell height, α_s is the layer split factor, and α_c is the layer collapse factor. [14].

Experimental equipment and methods

Figure-5 shows the measuring device of the cooling capacity of the cooling cycle used in these experiments. The test conditions are shown in Table-2. The stroke and frequency of the linear compressor were controlled by the power supply, and an oscilloscope and a powermeter are used to measure the location of the stroke and the phase between the current and the back electromagnetic force. The experiments were carried by LG Electronics [15].

RESULTS AND DISCUSSIONS

Variations of flow velocity with piston displacement

Figure-6 shows the velocity distribution of model-1 and model-2 when the piston angle in the second cycle is 118°. Right after the suction valve has been closed, the internal

Table-2. Test conditions for the refrigeration cycle.

Property	Value
Stroke	12.4 mm
Frequency	56.5 Hz
Suction temperature (T1)	25.0 °C
Condenser pressure (P2)	416,030 Pa
Evaporator pressure (P4)	48,550 Pa

pressure of the piston becomes higher than the inlet pressure by the flow inertia. Due to this pressure difference, the reverse flows of the maximum 8.5 m/s occurs in the case of Model-1 and also the reverse flows of the maximum 19.4 m/s occurs in the case of model-2. This is because model-2 generates larger flow inertia than model-1 due to its multi-stage expansion tubes and a muffler.

When the piston angle in the second cycle is 270°, the velocity distribution of model-1 and model-2 are shown in Figure-7. In the case of model 1, the maximum velocity of 50 m/s occurs at the Venturi tube of the inlet pipe and in the case of model-2, the maximum velocity of about 60 m /s occurs at the third expansion tube from the inlet. This also results from the fact that model-2 has higher pressure difference between the piston and the inlet in comparison with model-1. On the other hand, the convergence problem might occur since the flow velocity into the cylinder right after the opening of the suction valve is too high. This is because the movement of the suction valve was simplified so that the suction valve can be instantaneously fully open or closed. Therefore, in order to improve the convergence, the simulation was temporarily performed for 500 time steps with time step of 10^{-6} s.

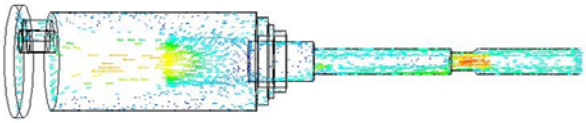

(a) Model-1

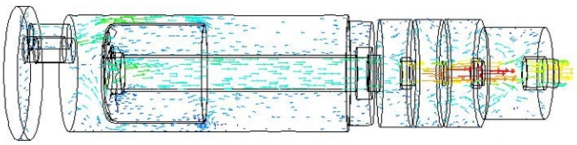

(b) Model-2

Figure-6. Velocity vectors for model-1 and model-2 at piston angle of 118°.

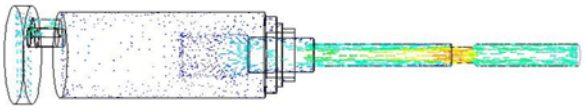

(a) Model-1

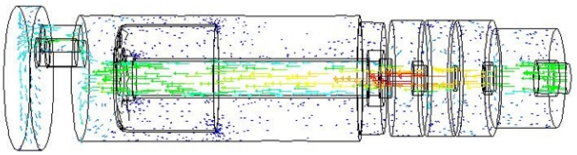

(b) Model-2

Figure-7. Velocity vectors for model-1 and model-2 at piston angle of 270°.

Variations of pressure with piston displacement

Figure-8 shows the variation of the cylinder pressure with the piston displacement for the second cycle. Model-1 indicates a higher pressure of up to 18.1% as compared to model-2 in compression process 1→2 as well as a higher pressure of up to 3.0% in expansion and suction process 4→1. This suggests that more refrigerant enters the cylinder in the case of model-1 since both models have same cylinder volume. This also serves to further increase the maximum pressure during the next compression process.

Figure-9 shows the variation of the pressure on the piston side surface of the suction valve with the piston angle for the second cycle. Model-2 shows relatively low pressure in comparison with model-1, except for the range from 54° to 180°. It is because model-2 generates larger flow resistance in comparison with model-1 due to the muffler and the multi-stage pipes inside the piston of model-2.

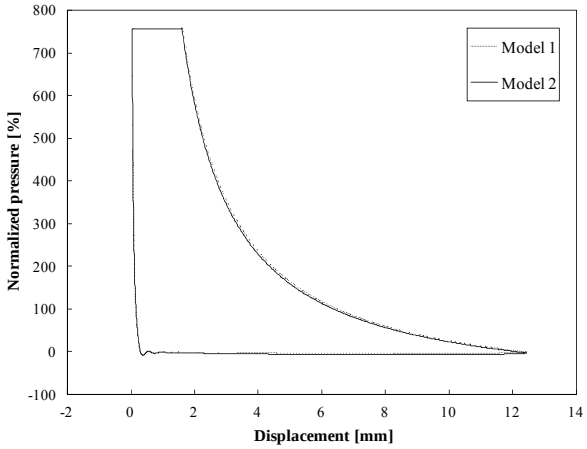

Figure-8. Variations of normalized cylinder pressure with piston displacement.

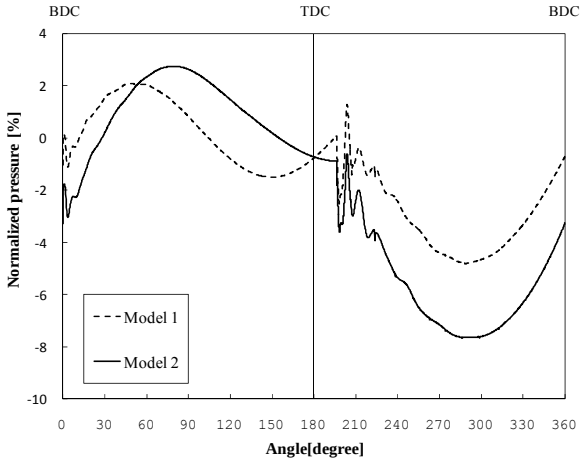

Figure-9. Variations of normalized pressure at the piston-side surface of the suction valve with piston angle.

After the suction valve opens, the pressure in model-2 drops about 3% more than model-1 at the piston angle of 324°, which causes greater pressure rise for the next compression process.

Variations of mass flow rate with piston displacement

Figure-10 shows the variation of the normalized mass flow rate at the compressor inlet with the piston angle. The mass flow rate is normalized by the cycle-average mass flow rate. The reverse flows are observed at the inlet during the compression process regardless of the model. The reverse flows occur between about 72.4° and 132.8° and the maximum normalized mass flow is 134% for model-1. For model-2, the reverse flows occur between about 78.5° and 199.9° and the maximum normalized mass flow is 199%. This suggests that the high pressure caused by the flow inertia prevents the inflow of refrigerant from the outlet of the evaporator. Also, it can be seen that the variation of mass flow rate by the flow inertia corresponds to that of pressure by the flow inertia.

Figure-10 shows the variation of the normalized mass flow rate of the suction valve with the angle of the piston for the second cycle. Although the difference of the mass flow rates between both models is very little, it can be seen that model-1 has higher refrigerant intake of about 2.4% in comparison with model-2. This is because model-1 has lower flow resistance than model-2. In particular, the difference of the mass flow rate between both models

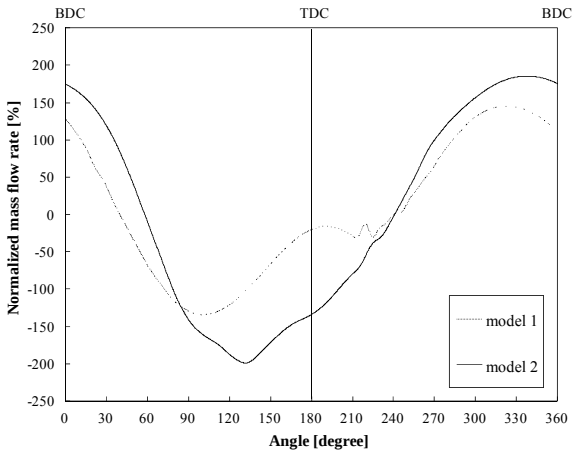

Figure-10. Variations of normalized mass flow rate at compressor inlet with piston angle.

Table-3. Comparison of normalized cooling capacity.

	Model-1	Model-2	Difference between Model-1 and model-2
Experiment	100.0%	98.5%	-1.6%
Numerical analysis	120.7%	117.8%	-2.4%
Difference between Exp. and Num.	20.7%	19.4%	0.8%

becomes prominent in the piston angle range of 240° to 300°, where the piston speed is the fastest. Model-1 shows a higher mass flow rate of 20 % than model-2 at the piston angle of about 251°.

Variations of compressor cooling capacity with the models

The variations of the cooling capacity of the compressor with the models are shown in Table-3. The cooling capacity was normalized by the measured cooling

capacity of model-1. First, the numerical cooling capacity is compared with the experimental value. For model-1, the numerical value is greater by 20.7% than the experimental value and by 19.4% for model-2. So the difference between both values is comparatively large. It is suggested that this difference results from the simplification of the valve behavior in the numerical analysis. Therefore, in order to predict the accurate cooling capacity, the accurate modeling for the behavior of the suction valve or the discharge valve is necessary, which requires FSI (Fluid-Structure Interaction) analysis.

Next, the comparison of the cooling capacity between the models is performed. By the experimental results, the cooling capacity of model-1 is greater by 1.6% than that of model-2. By the numerical simulations, the cooling capacity of model-1 is greater by 2.4% than that of model-1. Therefore, the numerical analysis shows a good agreement with the experiment. In conclusion, the numerical analysis model developed in this study can be successfully used for shape optimization of the linear compressor.

CONCLUSIONS

In this study, the 3-dimensional CFD model for the linear compressor was developed and verified through the experiments. Furthermore, the variations of flow velocity, pressure, mass flow rate and cooling capacity with the compressor models were examined. The conclusions obtained through this study are as follows:

a) By the numerical analysis, the internal pressure of the piston during the compression process is about 2% higher for model-2 than model-1, and the internal pressure during the expansion process is about 3% lower for model-2 than model-1. This is because model-2 has the muffler and the multi-stage expansion tubes in the piston that cause a greater pressure loss.
b) Model-2 shows not only 20% lower maximum mass flow rate but also 2 % smaller total mass flow compared to model-1. This is again due to the additional pressure drop by the muffler and the multi-stage expansion tubes.
c) The numerical predictions of cooling capacity are relatively large compared with the experimental values due to the simplification of the valve behavior. However, the numerical predictions for relative comparison of cooling capacity with compressor shape are in good agreement with the experimental results. Therefore, the numerical model developed in this study can be successfully used for optimizing the shape of the compressor for better performance.

In the future, a FSI analysis considering the behavior of the valve will be performed to improve the prediction accuracy of the cooling capacity for a linear compressor.

ACKNOWLEDGEMENTS

This research was supported by Basic Science Research Program through the National Research Foundation of Korea(NRF) funded by the Ministry of Education, Science and Technology (2011-0024805). In addition, this work was supported by the Human Resources Development program(No. 20134030200230) of the Korea Institute of Energy Technology Evaluation and Planning(KETEP) grant funded by the Korea government Ministry of Trade, Industry and Energy.

Nomenclature

h: Enthalpy [kJ/kg] or height [m]
k: Turbulence energy [J/kg]
m: Mass flow rate [kg/s]
P: Pressure [Pa]
Q_{CC}: Cooling capacity [W]
S_h: Volumetric heat source [W/m^3]
t: Time [s]
T: Temperature [K]
A: Layering facor
ε: Turbulence dissipation rate [J/kg·s]

Subscripts

avg: Average
c: Collapse
cc: Cooling capacity
s: Split

REFERENCES

[1] H. K. Lee, G. Y. Song, J. S. Park, E. P. Hong and W. H. Jung. 2000. Development of the Linear Compressor for a Household Refrigerator. Proceedings International Compressor Engineering Conference, Purdue University. pp. 31-38.

[2] H. Lee, S. H. Ki, S. S. Jung and W. H. Rhee. 2008. The Innovative Green Technology for Refrigerators Development of Innovative Linear Compressor. Proceedings International Compressor Engineering Conference, Purdue University.

[3] J. K. Kim, C. K. Roh, H. Kim and J. H. Jeong. 2011. An Experimental and Numerical Study on an Inherent Capacity Modulated Linear Compressor for Home Refrigerators. International Journal of Refrigeration. 34: 1415-1423.

[4] J. K. Kim and J. H. Jeong. 2013. Performance Characteristics of a Capacity-Modulated Linear Compressor for Home Refrigerators. International Journal of Refrigeration. 36: 776-785.

[5] H. Kim, C. K. Roh and J. K. Kim. 2009. An Experimental and Numerical Study on Dynamic Characteristic of Linear Compressor in Refrigeration

System. International Journal of Refrigeration. 31: 1536-1543.

[6] C. R. Bradshaw, E. A. Groll and S. V. Garimella. 2011. A Comprehensive Model of a Miniature-Scale Linear Compressor for Electronics Cooling. International Journal of Refrigeration. 34: 63-73.

[7] N. Chen, Y. J. Tang, Y. N. Wu, X. Chen and L. Xu. 2007. Study on Static and Dynamic Characteristics of Moving Magnet Linear Compressors. Cryogenics. 47: 457-467.

[8] N. C. Tsai and C. W. Chiang. 2010. Design and Analysis of Magnetically-Drive Actuator Applied for Linear Compressor. Mechatronics. 20: 596-603.

[9] Y. P. Yang and B. J. Huang. 1998. Fuzzy Control on the Phase and Stroke of a Linear Compressor of a Split-Stirling Cryocooler. Cryogenics. 38: 231-238.

[10] 2013. Ansys Fluent V14, Ansys Inc.

[11] J. K. Kim and J. H. Jeong. 2013. Performance Characteristics of a Capacity-Modulated Linear Compressor for Home Refrigerators. International Journal of Refrigeration. 36: 776-785.

[12] B. E. Launder and D. B. Spalding. 1974. The Numerical Computation of Turbulent Flows. Computer Methods in Applied Mechanics and Engineering. 3: 269-289.

[13] 2013. Thermodynamic and Transport Properties of Refrigerants and Refrigerant Mixtures Database V7.0, National Institute of Standards and Technology.

[14] Ansys. 2013. ANSYS FLUEN User's Manual Version 14.0, ANSYS Inc.

[15] LG electronics Inc., http://www.lge.co.kr.